ANALYSIS OF COMPOSITE DIELECTRIC METAMATERIALS USING INTEGRAL EQUATION TECHNIQUES

John Stevenson
University of Texas

ABSTRACT

We study numerically the electromagnetic scattering properties of three dimensional (3D), arbitrary shaped composite dielectric metamaterials. Using integral equation techniques, we first derive a surface integral equation formulation which produces well-conditioned matrix equation. To solve the obtained integral equations, we apply a Galerkin scheme and choose the basis and testing functions as Rao-Wilton-Glisson defined on planar patches. We then develop an algorithm to speed up the matrix-vector multiplications by employing the well-known method of moments (MoM) and the multilevel fast multipole algorithm on personal computer (PC) clusters. Some 3D numerical examples are presented to demonstrate the validity and accuracy of the proposed approach.

INTEGRAL EQUATION FORMULATION

Consider the case in figure 2 involving the problem of electromagnetic scattering by an arbitrary shaped, homogenous dielectric object B characterized by electrical properties (ε_i, μ_i) which is surrounded by an infinite medium having (ε_o, μ_o).

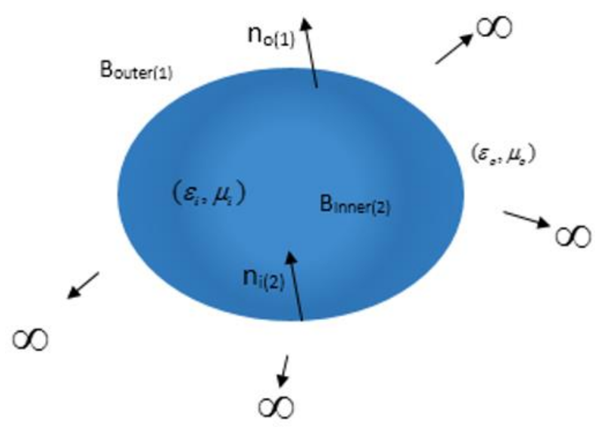

Using the equivalence principle, the inner and outer normal (N) and tangential (T) electric and magnetic fields can be considered as:

N-EFIE(l) $$\eta_l \hat{n}_l \times \Gamma\{\mathrm{J}_l\} - \hat{n}_l \times \mathrm{K}\{\mathrm{M}_l\} = -\hat{n}_l \times \mathrm{E}_l^{inc}$$

T-EFIE(l) $$\hat{n}_l \times \hat{n}_l \times \mathrm{K}\{\mathrm{M}_l\} - \eta_l \hat{n}_l \times \hat{n}_l \times \Gamma\{\mathrm{J}_l\} = (\hat{n}_l \times \hat{n}_l \times \mathrm{E}_l^{inc})_{\tan}$$

N-MFIE(l) $\hat{n}_l \times \mathrm{K}\{\mathrm{J}_l\} - \eta_l^{-1}\hat{n}_l \times \Gamma\{\mathrm{M}_l\} = -\hat{n}_l \times \mathrm{H}_l^{inc}$

T-MFIE(l) $-\hat{n}_l \times \hat{n}_l \times \mathrm{K}\{\mathrm{J}_l\} - \eta_l^{-1}\hat{n}_l \times \hat{n}_l \times \Gamma\{\mathrm{M}_l\} = (\hat{n}_l \times \hat{n}_l \times \mathrm{H}_l^{inc})_{\tan}$

In (1)-(4), $\hat{n}_l$ denotes the inner unit normal for l=i and outer unit normal for l=o, $\eta_l = \sqrt{\mu_l/\varepsilon_l}$ is the impedance of the host medium with $l = \{i(inner), o(outer)\}$, $(\mathrm{E}_l^{inc}, \mathrm{H}_l^{inc})$ denote the incident electric and magnetic fields respectively, and J_l and M_l are equivalent electric and magnetic currents on the surface of the object which are related to the total electric (E) and magnetic (H) fields as

$$\mathrm{J}_l(r') = \hat{n}_l \times \mathrm{H}(r')$$
$$\mathrm{M}_l(r') = \mathrm{E}(r') \times \hat{n}_l$$

The operators Γ and K operators are defined as

$$\Gamma\{\mathrm{X}\} = jk_l[\int_s \mathrm{X}(r')ds' + k_l^{-2}\int_s ds'\nabla'.\mathrm{X}(r')\nabla]\mathrm{G}_l(r,r')$$
$$\mathrm{K}\{\mathrm{X}\} = \int_s \mathrm{X}(r') \times \nabla'\mathrm{G}_l(r,r')ds'$$

Where $k_l = \omega\sqrt{\mu_l\varepsilon_l}$ is the wavenumber and we define

$$\mathrm{G}(\mathrm{r},\mathrm{r}') = \frac{e^{-jk_lR}}{4\pi R} \qquad (R = |r - r'|)$$

Which is the homogenous Green's function.

Among the various possibilities of combination of the normal and tangential electric and magnetic fields, the following mixed formulation is called the electric and magnetic current combined field integral equation (JMCFIE) [1, 2], i.e.

$$\begin{bmatrix} \sum_{l=1}^{2}\eta_l^{-1}\{\text{T-EFIE(l)}\} + \sum_{l=1}^{2}(-1)^{2l}\{\text{N-MFIE(l)}\} \\ \sum_{l=1}^{2}\eta_l\{\text{T-MFIE(l)}\} - \sum_{l=1}^{2}(-1)^{2l}\{\text{N-EFIE(l)}\} \end{bmatrix}$$

$$\begin{bmatrix} [Z_{11}]_{N\times N} & [Z_{12}]_{N\times N} \\ [Z_{21}]_{N\times N} & [Z_{22}]_{N\times N} \end{bmatrix} . \begin{bmatrix} \mathrm{J} \\ \mathrm{M} \end{bmatrix} = \begin{bmatrix} \eta_l^{-1}(\mathrm{E}^{inc})_{\tan} - \hat{n}_l \times \mathrm{H}^{inc} \\ \eta_l(\mathrm{H}^{inc})_{\tan} + \hat{n}_l \times \mathrm{E}^{inc} \end{bmatrix}$$

For a composite dielectric object involving B-1 regions $B_1, B_2, \ldots, B_n$ with constitutive parameters (ε_n, μ_n) located in a host medium (ε_0, μ_0), the surface integral equation can be written as

$$\begin{bmatrix} [\sum_{B=0}^{B-1} Z_{11,n}]_{N\times N} & [\sum_{B=0}^{B-1} Z_{12,n}]_{N\times N} \\ [\sum_{B=0}^{B-1} Z_{21,n}]_{N\times N} & [\sum_{B=0}^{B-1} Z_{22,n}]_{N\times N} \end{bmatrix} \cdot \begin{bmatrix} \mathrm{J} \\ \mathrm{M} \end{bmatrix} = \begin{bmatrix} \sum_{B=0}^{B-1} (\eta_l^{-1} (\mathrm{E}^{inc})_{\tan} - \hat{n}_l \times \mathrm{H}^{inc})_{1,n} \\ \sum_{B=0}^{B-1} (\eta_l (\mathrm{H}^{inc})_{\tan} + \hat{n}_l \times \mathrm{E}^{inc})_{2,n} \end{bmatrix}$$

DISCRETIZATION AND ITERATIVE SOLUTION

In order to discretize the surface integral equation , one popular choice is the Rao-Wilton-Glisson (RWG) basis function [3], which discretizes the surface of the dielectric object into small elements each of which is triangle. Figure 3 depicts an RWG function on a pair of triangles.

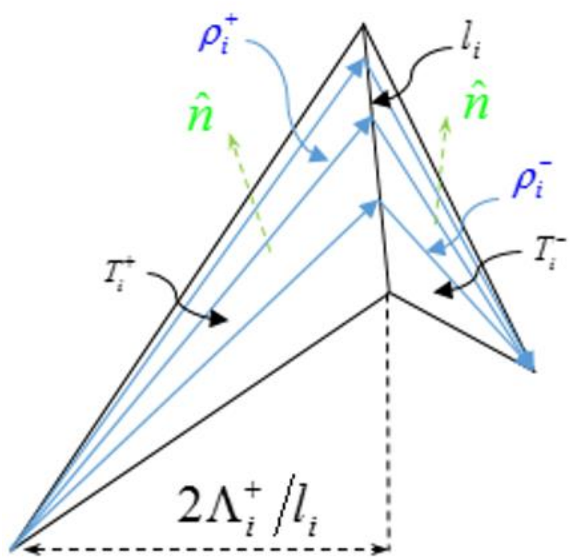

An RWG function

An RWG function associated with the i th edge can be defined as

$$\mathrm{f}_i(r) = \begin{cases} \frac{l_i \rho_i^+}{2\Lambda_i^+}, & r \in T_i^+ \\ -\frac{l_i \rho_i^-}{2\Lambda_i^-}, & r \in T_i^- \\ 0, & otherwise \end{cases}$$

Where l_i is the length of the main edge, $\Lambda_i^{\pm}$ is area of triangle $T_i^{\pm}$ associated with the edge, and ρ_i^+ and ρ_i^+ are respectively position vectors with respect to the free vertex of T_i^+ and T_i^- . Also note that in figure 3, the total charge is zero for each RWG function, ensuring that all edges of T_i^+ and T_i^- are free of line charges.

Discretization using RWG functions leads to the following:

$$\begin{bmatrix} \mathrm{TT_n} + \mathrm{NK_n} & \dfrac{1}{\eta_n}\left[\mathrm{NT_n} - \mathrm{TK_n}\right] \\ \eta_n\left[\mathrm{TK_n} \text{-} \mathrm{NT_n}\right] & \mathrm{TT_n} + \mathrm{NK_n} \end{bmatrix} \cdot \begin{bmatrix} \mathrm{J} \\ \mathrm{M} \end{bmatrix} = \begin{bmatrix} \mathrm{E}_{\psi,\mathrm{n}} \\ \mathrm{H}_{\psi,\mathrm{n}} \end{bmatrix}$$

In which discretized operators can be written as

$$\underset{n}{\overset{[p,q,r,s]}{\mathrm{TT}}} = \frac{\pm jk_n l_p l_q}{4\Lambda_{p,r}\Lambda_{q,s}} \int_{S_{p,r}} \rho^{+}_{p,r} dr \cdot \int_{S_{q,s}} \mathrm{G}_n(r,r')\rho^{-}_{q,s} dr' - \frac{\mp jk_n^{-1} l_p l_q}{\Lambda_{p,r}\Lambda_{q,s}} \int_{S_{p,r}} dr \cdot \int_{S_{q,s}} \mathrm{G}_n(r,r') dr'$$

$$\underset{n}{\overset{[p,q,r,s]}{\mathrm{NT}}} = \frac{\pm jk_n l_p l_q}{4\Lambda_{p,r}\Lambda_{q,s}} \int_{S_{p,r}} \hat{n}\times\rho^{+}_{p,r} dr \cdot \int_{S_{q,s}} \mathrm{G}_n(r,r')\rho^{-}_{q,s} dr' - \frac{\mp jk_n^{-1} l_p l_q}{2\Lambda_{p,r}\Lambda_{q,s}} \int_{S_{p,r}} \hat{n}\times\rho^{+}_{p,r} dr \cdot \int_{S_{q,s}} \nabla\,\mathrm{G}_n(r,r') dr'$$

$$\underset{n}{\overset{[p,q,r,s]}{\mathrm{NK}}} = \frac{\pm l_p l_q}{4\Lambda_{p,r}\Lambda_{q,s}} \int_{S_{p,r}} \hat{n}\times\rho^{+}_{p,r} dr \cdot \rho^{+}_{q,s} \times \int_{S_{q,s}} \nabla\,\mathrm{G}_n(r,r') dr'$$

$$\underset{n}{\overset{[p,q,r,s]}{\mathrm{TK}}} = \frac{\pm l_p l_q}{4\Lambda_{p,r}\Lambda_{q,s}} \int_{S_{p,r}} \rho^{+}_{p,r} dr \cdot \rho^{+}_{q,s} \times \int_{S_{q,s}} \nabla\,\mathrm{G}_n(r,r') dr'$$

In the far-field scattering electric field can be written as:

$$\mathrm{E}^{sca} = \frac{j\omega\mu_0}{4\pi}\left[\int_S \mathrm{J}(r') e^{-jk_0\cdot r'} dr' - \eta_0^{-1}\int_S \mathrm{M}(r') e^{-jk_0\cdot r'} dr'\right]$$

The discretization gives:

$$\begin{aligned}
\mathrm{E}^{sca} &= \frac{j\omega\mu_0}{4\pi}\left[\int_S \sum_{n=1}^{N} c_n^{\mathrm{J}} v_n^{\mathrm{J}}(r') e^{-jk_0\cdot r'} dr' - \eta_0^{-1}\int_S \sum_{n=1}^{N} c_n^{\mathrm{M}} v_n^{\mathrm{M}}(r') e^{-jk_0\cdot r'} dr'\right] \\
&= \pm\frac{j\omega\mu_0}{4\pi}\cdot\sum_{n=1}^{N} c_n^{\mathrm{J}} \sum_{q=1}^{2} \frac{l_n}{2\Lambda_{nq}} \int_S \rho^{+}_{n,q} e^{-jk_0\cdot r'} dr' \\
&- \frac{jk_0}{4\pi}\cdot\sum_{n=1}^{N} c_n^{\mathrm{M}} \sum_{q=1}^{2} \frac{l_n}{2\Lambda_{nq}} \int_S \rho^{+}_{n,q} e^{-jk_0\cdot r'} dr'
\end{aligned}$$

NUMERICAL RESULTS

The procedure described above is implemented for the solution composite dielectric metamaterials. In this section, the developed surface integral equation is analyzed by numerical examples. The process is implemented in MATLAB.

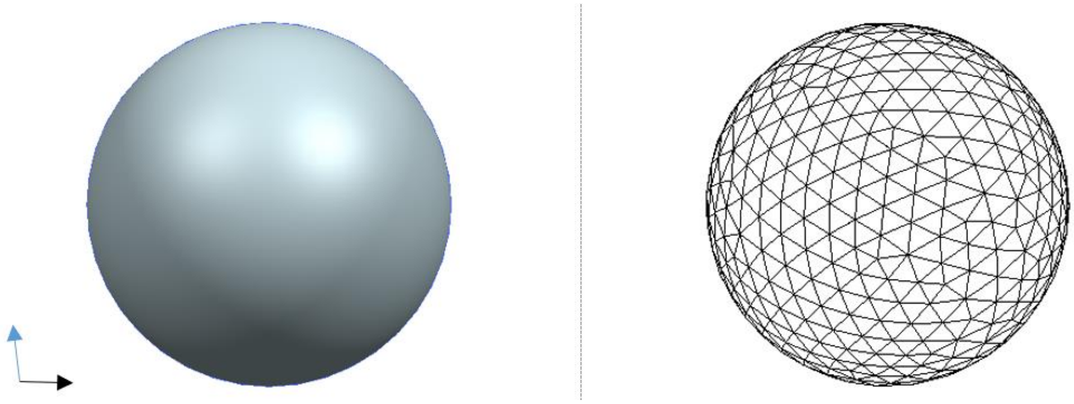

Sphere with 1 λ radius (b) triangulation with λ /6 mesh size

We first consider a simple case which involves the problem of plane wave scattering by a uniform dielectric sphere in free space. The sphere has a radius of $2\lambda_0$, where λ_0 is the free space wavelength.

NUMERICAL EXAMPLES

Current density on sphere using numerical solution of

$$\mathrm{J}(r,t) = \int_{-\infty}^{t} dt' \int d^3 r' \sigma(r-r', t-t')\, \mathrm{E}^{sca}(r', t')$$

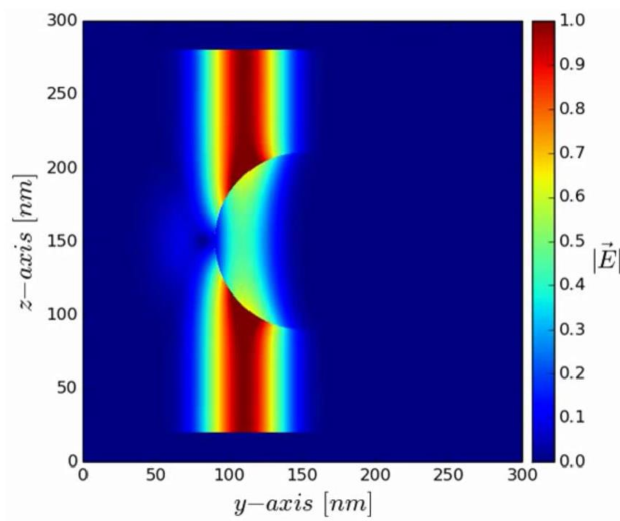

Readers can refer to the following papers for in depth theoretical analysis and device simulations in MEMS and optics [4-14].

REFERENCES

[I] P. Yla-Oijala and M. Taskinen, "Application of combined field integral equation for electromagnetic scattering by dielectric and composite objects," Antennas and Propagation, IEEE Transactions on, vol. 53, pp. 1168-1173, 2005.

[2] P. Yla-Oijala, et al., "Surface integral equation method for general composite metallic and dielectric structures with junctions," Progress In Electromagnetics Research, vol. 52, pp. 81-108, 2005.

[3] Chorsi, H. T., Lee, Y., Alù, A., & Zhang, J. X. (2017). Tunable plasmonic substrates with ultrahigh Q-factor resonances. Scientific reports, 7(1), 1-9.

[4] J. W. Massey, C. S. Geyik, M. Ball, P. Findell, and A. E. Yilmaz, "AustinMan electromagnetic voxels," http://bit.ly/AustinMan/, Mar.2011.
[5] T. Malas, F. Wei, J. Massey, C. S. Geyik, and A. E. Yilmaz, "Application of AIM to high-resolution bioelectromagnetics simulations," in *Proc. Appl. Comp. Electromagnetics Symp.*, pp. 558- 563, Mar. 2011.
[6] A. Brandt, "Multilevel computations of integral transforms and particle interactions with oscillatory kernels," *Comp. Phys. Comm.,* vol. 65, pp.24-38, 1991.
[7] Chorsi, Hamid T., and Stephen D. Gedney. "Efficient high-order analysis of bowtie nanoantennas using the locally corrected Nyström method." Optics express 23.24 (2015): 31452-31459.
[8] J. R. Phillips and J. K. White, "A precorrected-FFT method for electrostatic analysis of complicated 3-D structures," *IEEE Trans. CAD*, vol. 16, no. 10, pp. 1059-1072, Oct. 1997.
[9] Chorsi, Meysam T., and Hamid T. Chorsi. "Modeling and analysis of MEMS disk resonators." Microsystem Technologies 24.6 (2018): 2517-2528.
[10] Chorsi, Hamid T., Meysam T. Chorsi, and Stephen D. Gedney. "A conceptual study of microelectromechanical disk resonators." IEEE Journal on Multiscale and Multiphysics Computational Techniques 2 (2017): 29-37.
[II] D. Schobert and T. F. Eibert, "A multilevel interpolating fast integral solver with fast Fourier transform acceleration," in *Proc. URSI Int. Symp. Electromag. Theory,* Aug. 2010, pp. 520-523.
[12] Chorsi, Hamid T., and John XJ Zhang. "Apertureless near-field scanning probes based on graphene plasmonics." IEEE Photonics Journal 9.1 (2017): 1-7.
[13] Chorsi, Hamid T., and John XJ Zhang. "Apertureless near-field scanning probes based on graphene plasmonics." IEEE Photonics Journal 9.1 (2017): 1-7.
[14] K. Yang, F. Wei, and A. E. Yilmaz, "A multigrid enhanced precorrected FFT/AIM algorithm for multiscale integral equation analysis," in *10th Int. Workshop Finite Elements Microw. Eng.,* New
Hampshire, US, Oct. 2010.